Comparing Radical Diffusion Crossover Phenomena in Alcohols and Alkanes

Jakov Slade[†], Dalibor Merunka,*[,†] and Miroslav Peric[‡]

[†]Division of Physical Chemistry, Ruđer Bošković Institute, Bijenička cesta 54, HR-10000 Zagreb, Croatia

[‡]Department of Physics and Astronomy, California State University, Northridge, Northridge, California 91330, United States

March 14, 2023

*Corresponding author. E-mail: merunka@irb.hr, Tel: +3851-4561-136

Abstract

We applied electron spin resonance (ESR) to study tracer diffusivities of a nitroxide radical at various temperatures in the normal alkanes (octane to tridecane) and alcohols (methanol to 1-octanol). We studied and compared radical diffusivities in these liquids because their molecules are similar, but alcohols exhibit heterogeneous structures due to the hydrogen bonding of hydroxyl groups, which is absent in alkanes. The crossover temperature behavior of radical diffusivities was found in all liquids by relating radical diffusivities and solvent self-diffusivities. This finding evidences the transformation from a single-molecule diffusion process into a collective process upon temperature lowering. However, the crossover behavior strongly differs in alcohols and alkanes, indicating that the heterogeneous structure of alcohols affects the radical diffusion crossover.

Keywords: tracer diffusivity; self-diffusivity; nitroxide radicals; electron spin resonance; monohydroxy alcohols; heterogeneous structure

1. Introduction

There is a theoretical and practical interest in studying the translational diffusion of solvent molecules (self-diffusion) and diluted solute molecules (tracer diffusion) in neutral molecular liquids and ionic liquids [1-4]. When the solute molecule is a stable free radical, its diffusion can be studied by electron spin resonance (ESR) spectroscopy [5-9]. Since the relative motion of solvated radicals modulates spin interactions between them, the ESR spectrum of radicals depends on their diffusion coefficient (diffusivity). Information about the radical diffusivity is obtained by measuring the shape changes of the ESR spectrum with radical concentration.

Diffusion in glass-forming liquids generally exhibits two crossover phenomena above the glass transition temperature T_g. These are the Stokes-Einstein (SE) violation phenomenon, which appears in the supercooled state below the temperature $T_c \approx 1.2T_g$, and the Arrhenius crossover phenomenon, which appears below the higher temperature T_A around or above the melting temperature T_m [10-12]. The first phenomenon denotes a significant enhancement of diffusivity over that predicted by the SE law, ascribed to the onset of spatially correlated and heterogeneous dynamics at T_c [10,11]. The latter phenomenon denotes a change from the Arrhenius temperature dependence of diffusivity above T_A into a stronger non-Arrhenius one below T_A, ascribed to the onset of correlated and cooperative diffusive motion of molecules at T_A [12]. The Arrhenius crossover phenomenon was also detected in the temperature dependences of relaxation time and viscosity [13].

ESR study of the tracer diffusion of a radical in six glass-forming solvents showed the crossover behavior of radical diffusivities when they were related to self-diffusivities [14]. The radical diffusivities, being lower than the self-diffusivities at high temperatures, approach the self-

diffusivities by the temperature lowering through the crossover region between $T_{cr}+\Delta$ and $T_{cr}-\Delta$, where T_{cr} is the crossover temperature, and 2Δ is the crossover temperature width. The Arrhenius crossover temperatures T_A estimated from experimental viscosities were found to be close to the onset temperatures of radical diffusion crossover $T_{on}=T_{cr}+\Delta$ in all studied liquids except ethanol [14]. This finding indicates the same origin of both crossover phenomena, while the exception of ethanol, where T_{cr} is significantly higher than T_A, was tentatively related to the existence of heterogeneous nanoscopic structures in monohydroxy alcohols.

The heterogeneous structure in alcohols consists of polar domains with hydrogen-bonded hydroxyl groups and non-polar domains with alkyl tails, which is manifested in diffraction spectra by the presence of a pre-peak in addition to the main peak [4,15]. Also, the structural dynamics of monohydroxy alcohols exhibit a structural α-relaxation, which is attributed to the dynamics of alkyl chains, and much slower Debye relaxation, which is attributed to the dynamics of hydrogen-bonded clusters [15,16]. Like monohydroxy alcohols, ionic liquids (ILs) with long alkyl chains on the cation exhibit a nanoscopic structure that contains less mobile polar domains with charged molecular parts and more mobile non-polar domains with alkyl chains [3,4].

The possible influence of the nanostructure in alcohols and ILs on tracer and self-diffusion is an interesting question for diffusion studies in these liquids [3,4,15,17-20]. The tracer diffusion study in ILs revealed that neutral tracers exhibit positive and charged tracers negative deviations of diffusivities from those predicted by the SE relation [3], ascribed to the effect of nanostructure [18]. The positive effect of non-polar alkyl domains on neutral tracer diffusivity was also found by measuring tracer diffusivity in 1-alkyl-3-methylimidazolium ILs as a function of alkyl chain length [19,20]. Whereas the cation and anion self-diffusivities decrease with alkyl chain length,

the tracer diffusivity of the nitroxide radical shows only a negligible decrease for long chains [19] and, even more surprising, the tracer diffusivity of xenon increases with alkyl chain length [20]. The reported negative effect of nanostructure on ionic mobility in ILs is a sharp decrease of ionic conductivity in tetraalkylammonium ILs when the volume fraction of alkyl chains exceeds 40% [21]. The nanostructure in monohydroxy alcohols was reported to affect the distribution and mobility of catalyst $CuCl_2$ [22] and to cause a non-monotonic temperature dependence of the conductivity of probe ions [23].

Here, we report an ESR study of the temperature behavior of diffusion of nitroxide radical pDTEMPONE (perdeuterated 2,2,6,6-tetramethyl-4-oxopiperidine-1-oxyl) in the normal alkanes octane to tridecane (C8-C13) and the normal alcohols methanol to 1-octanol (C1OH-C8OH). We studied pDTEMPONE radicals labeled with ^{14}N and ^{15}N isotopes (^{14}N- and ^{15}N-pDTEMPONE) with different ESR spectra but practically equal diffusivities. Studying radical diffusion in alkanes is interesting because they are not glass-forming liquids and have similar molecules as alcohols but do not exhibit heterogeneous structures. Hence, comparing radical diffusion in these two types of liquids could reveal the effects of heterogeneous structure.

2. Materials and methods

The stable free radicals ^{14}N-pDTEMPONE (99 atom % D) and ^{15}N-pDTEMPONE (98 atom % D, 99 atom % ^{15}N) were purchased from CDN Isotopes and used as received. The purities of pDTEMPONE radicals were estimated using solutions of Fremy's salt radicals as standards [14]. Liquid alkanes were from Alfa Aesar except for undecane, which was from Sigma Aldrich. The alcohols were from Kemika (methanol and ethanol), T.T.T. (1-propanol and 1-butanol), and

Alfa Aesar (1-pentanol to 1-octanol). Stock solutions of pDTEMPONE were prepared by weight in all solvents, and then they were diluted to 12 solutions with nearly equally spaced concentrations, which were determined by weighing. Just before ESR measurements, the solutions were drawn into 5-μL capillaries and sealed at the lower end by Haematocrit sealing compound, while the upper end was left open.

ESR spectra were recorded with a Varian E-109 X-band spectrometer upgraded with a Bruker microwave bridge and a Bruker high-Q cavity. The sample temperature was controlled by a Bruker variable temperature unit and measured with a thermocouple using an Omega temperature indicator. The thermocouple tip was positioned at the top of the active region of the ESR cavity to avoid reducing the cavity quality factor. All samples were measured in steps of 5 K in various temperature ranges depending on the solvent. The radical concentrations were corrected at measured temperatures by taking into account the estimated purities of radicals and the temperature dependences of solvents' densities from the literature.

In order to determine radical diffusivity, the measured ESR spectra were analyzed by a previously described procedure [7,9,14,19,24]. The procedure is shortly described in the following text and Appendix A of Supplementary material. In the first step, all ESR spectra were fitted to the theoretical ESR spectral function for solutions of ^{14}N- and ^{15}N-labeled radicals with spin interactions (Fig. A.1). The second step was to analyze relevant ESR parameters that depend on radical diffusivity and determine their linear concentration coefficients at each temperature. The analyzed ESR parameters were the spin coherence-transfer rate Λ and the average spin dephasing rate Γ, corresponding to the average width of hyperfine lines. The best-fit values of these ESR parameters were fitted to the linear function of radical concentration at each temperature. The concentration coefficients were determined as the slopes of fitting functions (Fig. A.1).

Determined concentration coefficients at a given temperature were compared to their theoretical dependences on the radical diffusivity D_T (Fig. A.2). The theoretical dependences were calculated by modeling dissolved radicals as continuously diffusing hard spheres and applying the formalism of the kinetic equations for the spin density matrices of radicals [6,9,14,19,24,25].

Since the concentration coefficient Λ was found to be the best parameter for the calculation of radical diffusivity [9], the diffusivities obtained from this coefficient were used in the averaging for the whole measured temperature range. On the other hand, the concentration coefficient Γ was found to saturate at low radical diffusivity [5,9], and the diffusivities obtained from this coefficient were taken into account for values higher than $25 \cdot 10^{-11}$ $m^2 s^{-1}$ (Fig. A.3). The final diffusivity of the pDTEMPONE radical was calculated as the average value of the diffusivities obtained from the concentration coefficients of ^{15}N- and ^{14}N-labeled radicals, which show similar values (Fig. A.3).

3. Results and discussion

The diffusivity of pDTEMPONE is presented as a function of temperature in alkanes (Fig. 1) and alcohols (Fig. 2). In order to relate radical and solvent diffusivities, we collected self-diffusivity data from the literature (Appendix B of Supplementary material) and determined the temperature dependence of self-diffusivity by fitting data to the Arrhenius or Vogel-Fulcher-Tammann laws (Figures B.1 and B.2). The best-fit parameters are given in Table B.1, and the fitted values of self-diffusivities $D_S(T)$ are drawn in Fig. 1 for alkanes and Fig. 2 for alcohols.

Figure 1. Radical diffusivities (symbols), fitted self-diffusivities (dotted lines), and radical diffusivity fits to Eq. (1) (full lines) versus temperature in alkanes.

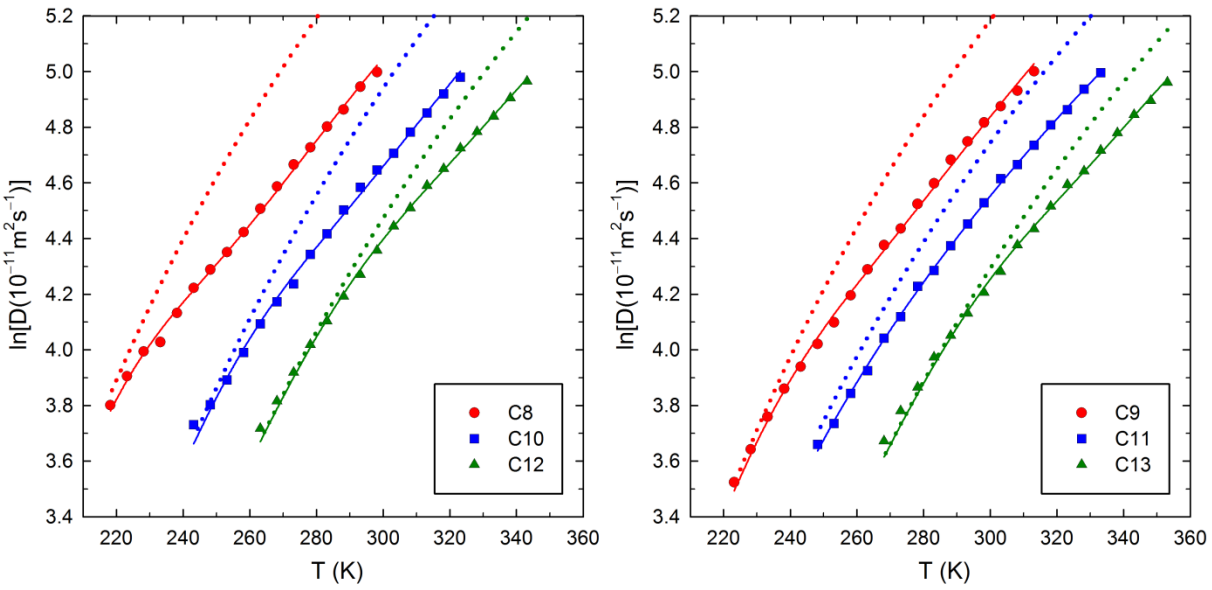

Using the fitted self-diffusivities $D_S(T)$, the temperature dependences of the tracer diffusivities of radical $D_T(T)$ were fitted to the relation:

$$D_T(T) = D_S(T)\left[R_H p_1 + R_L(1-p_1)\right];\ p_1 = \left[1+\exp\left(\frac{2T_{cr}}{\Delta}\frac{T_{cr}-T}{T}\right)\right]^{-1}, \qquad (1)$$

where R_H and R_L are the tracer to self-diffusivity ratios at high and low temperatures, respectively, T_{cr} is the crossover temperature and Δ is half the crossover temperature width. Eq. (1) with R_L=1 was proposed to describe the crossover behavior of the tracer diffusion of a radical in six glass-forming solvents [14]. Since $D_T(T)$ in the alkanes from C8 to C13 also exhibits the crossover toward $D_S(T)$ at low temperatures (Fig. 1), $D_T(T)$ in alkanes was fitted to Eq. (1) with the parameter

R_L fixed to 1. The resulting $D_T(T)$ fits are drawn in Fig. 1, and the best-fit values of parameters are written in Table B.2.

Figure 2. Radical diffusivities (symbols), fitted self-diffusivities (dotted lines), and radical diffusivity fits to Eq. (1) (full lines) versus temperature in alcohols.

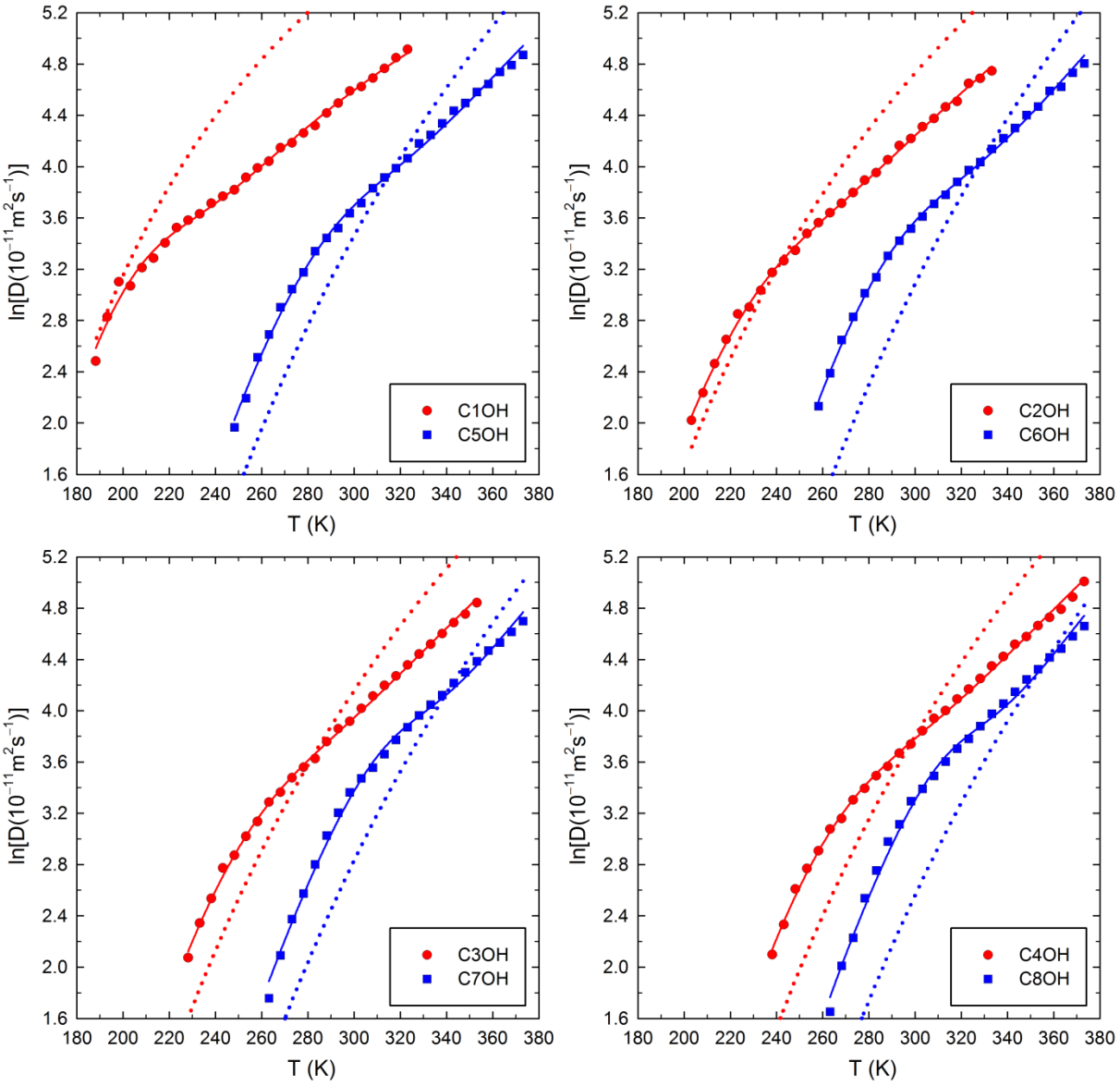

The fact that the tracer to self-diffusivity ratio $R_{TS}(T)=D_T(T)/D_S(T)$ increases from $R_H<1$ at high temperatures to $R_L=1$ at low temperatures was taken as evidence that the elementary diffusion process in glass-forming liquids becomes a more collective process upon cooling [14]. As more molecules participate in the elementary diffusion process upon cooling, the difference in size and mass of a participating radical molecule has a lower effect on the rate of this process, which causes less difference between the radical and self-diffusivities. This crossover from individual to collective diffusion process was quantified by the probabilities that one molecule participates in a given diffusion process as a single entity or part of collective rearrangements, which are given by p_1 and $1-p_1$, respectively. The probability $p_1(T)$ decreases by cooling, and its form in Eq. (1) was proposed by assuming a two-state (TS) model for the participation of a molecule in the individual or collective diffusion process [14]. When comparing an isolated diffusing molecule and a molecule participating in the collective process in a crowded environment, the first one requires extra energy [26], corresponding to the energy difference $E_{TS}=2k_BT_{cr}^2/\Delta$ in the TS model. On the other hand, the collective process demands coherent movements of participating molecules, which increases the rarity of this process [26]. This effect was modeled as the extra entropy cost $S_{TS}=E_{TS}/T_{cr}$ in the TS model for the molecule participating in the collective process.

The new result here is that the tracer diffusion in alkanes, which are not glass-forming liquids, exhibits the same crossover behavior. The same behavior can also be seen for the alcohols C1OH and C2OH, where $D_T(T)$ approaches $D_S(T)$ at low temperatures (Fig. 2). However, $D_T(T)$ in the alcohols with the number of carbon atoms in the alkyl chain n higher than 2 significantly exceeds $D_S(T)$ at low temperatures (Fig. 2). Therefore, $D_T(T)$ in all alcohols were fitted to Eq. (1) with the free parameter R_L. The resulting fits of $D_T(T)$ are drawn in Fig. 2, and the best-fit values of parameters are written in Table B.2. The peculiar behavior of the ratio $R_{TS}(T)$ for the alcohols

C*n*OH with $n>2$, which increases from $R_H<1$ at high temperatures to $R_L>1$ at low temperatures, needs further explanation. We propose that this unexpected behavior in the alcohols originates in their heterogeneous structure composed of polar domains with hydroxyl groups and non-polar domains with alkyl tails (Fig. 3).

Figure 3. Schematic illustration of a heterogeneous structure and an example of collective diffusion process in 1-pentanol. The shaded polar domains contain aggregated hydroxyl groups (balls) mostly linked with hydrogen bonds (dotted lines). The radical (blue) and four pentanol molecules (red) participate in the diffusion process, and their configurations are shown before (left panel) and after (right panel) the process. Molecules 1-3 participate by alkyl chain rotation about the hydrogen-bonded hydroxyl group, while molecule 4 participates, as a whole, by breaking the hydrogen bond with one molecule and forming it with another one.

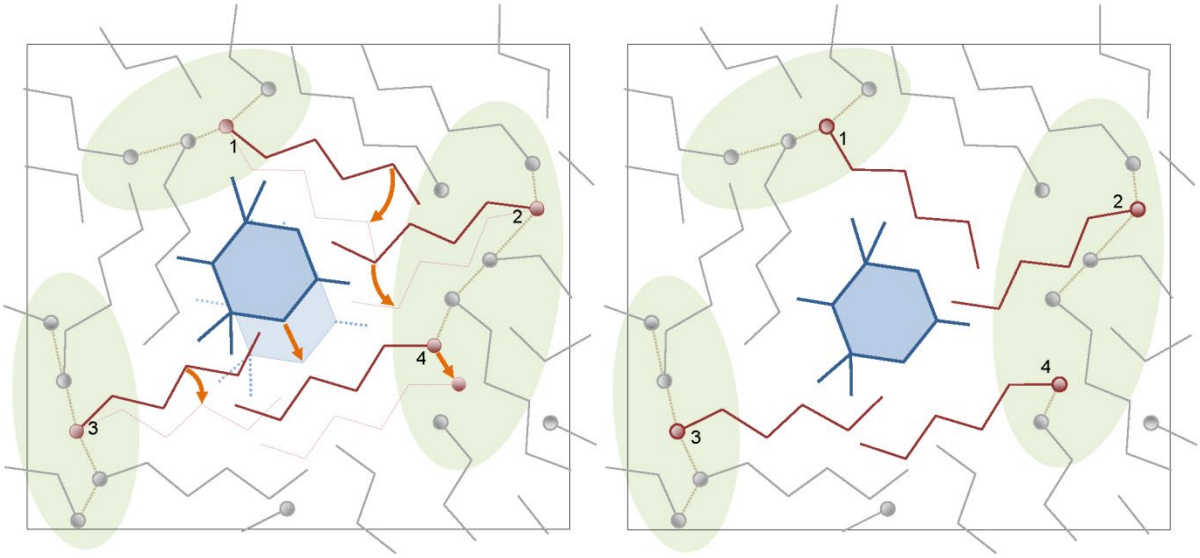

Experimental results showed that the pre-peak in diffraction spectra shifts to lower momentum transfers as the alkyl chain length n increases, which was ascribed to the increase of average distance between polar domains [15,16]. This implies that a radical molecule's probability of being in the non-polar domains increases with n. As non-polar domains increase in size with n over the size of the radical molecule, the radical in these domains becomes more dominantly surrounded by alkyl chains. By comparing NMR and dielectric measurements in alcohols, it was found that the correlation time of hydroxyl groups τ_{OH} is significantly shorter than the Debye relaxation time τ_D, but that τ_{OH} is significantly longer than the correlation time of alkyl chains τ_{alkyl}, which matches with the structural relaxation time τ_α [15,27-29]. The higher mobility of alkyl chains compared to the hydroxyl groups, which is implied by the inequality $\tau_{alkyl} \approx \tau_\alpha < \tau_{OH}$, was interpreted in a way that the hydroxyl groups are immobile during the period they participate in hydrogen-bonded chainlike aggregates, while the alkyl chains can move about backbones of these aggregates (Fig. 3). By calculating the hydrodynamic radius of the translationally diffusing object in alcohols from the SE relation and measured self-diffusivity data, it was concluded that the diffusing object is an individual molecule and not a whole hydrogen-bonded aggregate [15,27-29]. This finding was rationalized in the transient chain model, according to which the hydrogen-bonded chains move and reorient by successive detachments of bonded molecules from one end of the chain and attachments of unbonded molecules to the other end of the chain [27].

Following all the above findings and interpretations, we can set a simple picture in which alkyl chains mainly perform locally restricted diffusion about temporally fixed hydroxyl groups. At the same time, the long-range self-diffusion of the whole alcohol molecule is governed by repeated detachments of its hydroxyl group from one hydrogen-bonded chain and reattachments to another one (Fig. 3). By assuming that the time scale of the local diffusion process is about

$\tau_{\mathrm{alkyl}} \approx \tau_\alpha$ and the time scale of the self-diffusion process is about τ_{OH} [27,29], the local diffusivity of alkyl chains D_{loc} relates to the self-diffusivity D_S as $D_{loc}/D_S \approx \tau_{\mathrm{OH}}/\tau_\alpha$. Since τ_{OH} was found to be 5 to 10 times higher than τ_α at low temperatures in C4OH [15,27], the low-temperature D_{loc} is expected to be much higher than D_S. This implies that the collective diffusion process, presumably the prevailing process at low temperatures, includes, on average, more alkyl-chain displacements contributing mainly to D_{loc} than hydroxyl-group detachments contributing to D_S (Fig. 3). In this picture, the tracer diffusivity of radical D_T depends on how the probability of a radical participating in the collective diffusion process is related to the corresponding participation probabilities of alkyl chains and hydroxyl groups. A simple estimate is that the participation probability of the radical depends on its position within the heterogeneous structure: the radical within the polar domain has a participation probability close to that of the hydroxyl group. In contrast, the radical within the non-polar domain has a participation probability close to that of the alkyl chain. The estimate implies that the low-temperature radical diffusivity in alcohols satisfies $D_T \approx \phi D_S + (1-\phi) D_{loc}$, where ϕ is the probability of a radical to be in the polar domain. At the same time, the low-temperature ratio $R_L = D_T/D_S$ satisfies $D_{loc}/D_S > R_L > 1$, which is in accordance with the experiment (Table B.2 and Fig. 4a). The fact that R_L increases with alkyl chain length n (Table B.2 and Fig. 4a) agrees with the previous assumption that probability of a radical to be in the non-polar domains increases with n. The ratio $\tau_{\mathrm{OH}}/\tau_\alpha$ was found to decrease with temperature and reaches unity at some temperature, which is about room temperature in C4OH [15] and about 330 K in 2-ethyl-1-hexanol [29]. According to our picture, we expect that $D_T \approx D_S \approx D_{loc}$ will be satisfied close to this temperature. By inspecting Figs. 2 and 4, we can see that the ratio $R_{TS} = D_T/D_S$ in C4OH crosses unity about room temperature, according to this expectation.

Figure 4. (a) Various diffusivity ratios versus the number of carbon atoms n in alcohols: R_L and R_H are the best-fit values of tracer to self-diffusivity ratio D_T/D_S at low and high temperatures, respectively, R_{TS}(SE) is expected D_T/D_S from SE law, R_{TS}(25°C) is measured D_T/D_S at 25°C, and R_{TSE}(25°C) is the ratio between measured and SE tracer diffusivities D_T/D_T(SE) at 25°C. (b) Characteristic temperatures T_{ch} normalized to the melting temperatures T_m versus n in alcohols (blue) and alkanes (red): the radical diffusivity crossover temperatures T_{cr}/T_m (circles) with error bars that mark the crossover regions from $(T_{cr}-\Delta)/T_m$ to $(T_{cr}+\Delta)/T_m$, the Arrhenius crossover temperatures T_A/T_m from the viscosity fits (squares), and the temperatures T^*/T_m obtained from equation $\eta(T^*)$=1.5 mPa·s for alcohols (stars).

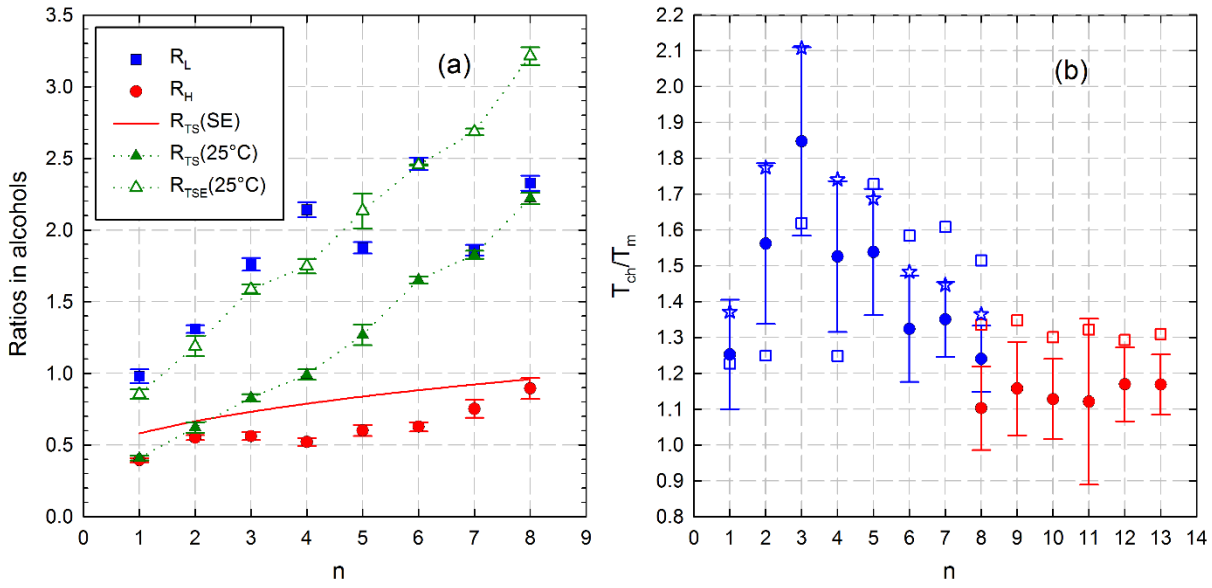

The tracer to self-diffusivity ratio R_{TS} in alcohols reaches the value of R_H<1 at the highest temperatures (Table B.2, and Figs. 2 and 4a). This fact can be ascribed to the domination of individual diffusion processes at these temperatures because the different sizes and masses of

radical and solvent molecules are expected to affect the rate of the individual process more than that of the collective one. By assuming that in this case, we can apply the SE law for tracer diffusivity:

$$D_T(\mathrm{SE}) = \frac{k_\mathrm{B}T}{6\pi\eta r_T} \qquad (2)$$

where r_T is the radius of the tracer molecule and η is the viscosity of the solvent. The expected tracer to self-diffusivity ratio is $R_{TS}(\mathrm{SE})=r_S/r_T$, where r_S is the radius of the solvent molecule. In our case, the radii of tracer and solvent molecules are calculated from the van der Waals volumes obtained by the fast-calculation method [30], assuming spherical molecular shapes. The obtained ratios R_{TS}(SE) for alkanes and alcohols are presented in Table B.2, while R_{TS}(SE) for alcohols are drawn in Fig. 4a. The agreement between R_{TS}(SE) and R_H is satisfactory because R_{TS}(SE) correctly predicts the value $R_H<1$ and also reproduces the weak dependence of R_H on alkyl chain length n (Fig. 4a). Summarizing whole discussion about the peculiar behavior of $R_{TS}(T)$ in the alcohols with $n>2$, we proposed that its high-temperature value $R_H<1$ reflects the diffusion governed by single-molecule processes, which is satisfactorily described by the SE law, while its low-temperature value $R_L>1$ reflects the diffusion governed by collective processes, which is strongly affected by the heterogeneous structure of alcohols with different mobility regions.

Because of practical interest in studying tracer and self-diffusion close to room temperature, we analyzed the ratios $R_{TS}=D_T/D_S$ and $R_{TSE}=D_T/D_T(\mathrm{SE})$ at 25°C for each studied alcohol (Fig. 4a). We calculated R_{TSE} by Eq. (2), using the radical radius of 3.5 Å and the viscosities calculated at 25°C from the power-law relations in Ref. [31]. As expected, the ratio R_{TS} strongly increases with n from R_H to R_L due to the crossover behavior of radical diffusivity (Fig. 4a). The ratio R_{TSE}, being close to one for C1OH, increases with n by a similar rate as R_{TS}, which means

that deviations from the SE law at room temperature also reflect the crossover behavior of radical diffusivity (Fig. 4a). Experimental room-temperature diffusivities of neutral solutes in various solvents exhibit increasing positive deviations from the SE law as the relative size between the solute and solvent molecules decreases [3,32,33]. Additionally, this deviation from the SE law depends much more strongly on the relative solute-to-solvent size in the alcohol solvents than non-polar ones [3,32,33]. Our results indicate that the reason for the stronger relative size dependence of the deviation in alcohols could be the stronger temperature crossover of solute diffusivity in alcohols due to the effect of heterogeneous structure.

As we did in the previous study of radical diffusion in six glass-forming solvents [14], we estimated the Arrhenius crossover temperatures T_A for the studied alcohols and alkanes (Appendix C of Supplementary material) from their experimental viscosity data (Fig. C1). The viscosities were fitted to Eq. (C1) with the parabolic non-Arrhenius term, which was previously applied to analyze metallic liquids' diffusivities [12], and the obtained best-fit parameters are written in Table C1. In order to compare the obtained temperatures T_A with the temperature regions of radical diffusion crossover, extending between $T_{cr}-\Delta$ and $T_{cr}+\Delta$, all characteristic temperatures in alcohols and alkanes are normalized to the melting temperatures T_m (Table B.2) and presented as a function of the number of carbon atoms n in Fig. 4b. The ratio T_A/T_m was considered in various glass-forming and crystallizing liquids as an indicator for the glass-forming ability of a particular liquid [34]. It was found that $T_A/T_m<1.02$ holds in crystallizing liquids, while this ratio becomes higher in glass-forming liquids, being in the range of $1.05<T_A/T_m<1.55$. This result was ascribed to locally favored structures that appear in liquids below the Arrhenius crossover temperature T_A. It was supposed that the local structures below $T_A>T_m$ in glass-forming liquids are inconsistent with long-range crystalline order and prevent crystallization below T_m. On the other hand, the local structures

below $T_A \approx T_m$ in crystallizing liquids were supposed to conform to long-range crystalline order and promote crystallization. It can be seen (Fig. 4b) that our results agree with these arguments because the studied alkanes, as crystallizing liquids, exhibit lower ratios T_A/T_m and T_{cr}/T_m than the studied alcohols, which are glass-forming liquids [35]. Also, it is known that glass-forming liquids with hydrogen bonds exhibit a higher ratio T_A/T_g than other molecular glass-forming liquids [12]. Hence, hydrogen bonding can be an additional reason why studied alcohols exhibit higher ratios T_A/T_m and T_{cr}/T_m than studied alkanes.

The estimated Arrhenius crossover temperatures T_A in all studied alkanes are close to the onset temperatures of radical diffusion crossover $T_{on}=T_{cr}+\Delta$, indicating the same origin of both crossover phenomena (Fig. 4b). Among alcohols, the coincidence between T_A and T_{on} was found for C5OH, while T_A is much lower than T_{on} for lower alcohols (n<5) and T_A is significantly higher than T_{on} for higher alcohols (n>5). To examine the source of the discrepancy between T_A and T_{on} in alcohols, we checked the values of T_A from our viscosity analysis against those from other measurements. The onset temperature in C2OH has a much higher value T_{on}=284 K (Table B2) than the value T_A=199 K (Table C1), which is practically equal to the value T_A=200 K obtained from the analysis of the true α-relaxation time [36]. In C3OH, the value T_{on}=311 K is also much higher than T_A=238 K, and the latter value is even higher than the value T_A=182 K obtained from the frequency of a dielectric-loss peak in C3OH [34,37], and the value T_A=199 K obtained from neutron scattering measurements of structural α-relaxation in isomeric 2-propanol [16]. We can conclude that low values of T_A from our viscosity analysis in C2OH and C3OH correspond to the values of T_A obtained from the analysis of structural α-relaxation, which is attributed to alkyl-chain dynamics.

It should be said that the high values of T_{on} in C2OH and C3OH could not be reproduced by the values of T_A from our viscosity analysis because viscosities were analyzed below 238 K in C2OH and 273 K in C3OH (Fig. C1 and Table C1). The reason for limited analysis is a downward deviation of viscosities from Arrhenius law above these temperatures, which could not be accounted for by the fitting formula, Eq. (C1). This high-temperature non-Arrhenius behavior was noticed above about 250 K in the temperature derivative analysis of dynamical quantities in C2OH and C3OH [37]. The same behavior was also noticed in the study of the temperature dependence of Debye relaxation time $\tau_D(T)$ in all alcohols studied here, where it was attributed to the thermal destabilizing effect on hydrogen-bonded chains at high temperatures [28]. This thermal effect could cause anomalous temperature behavior detected in C3OH above about 250 K for the dielectric strength of Debye relaxation and the absorbance ratio of near-infrared bands that correspond to weakly and strongly hydrogen-bonded OH groups [38]. In this study [38], the anomalous temperature behavior was not detected for corresponding quantities in dihydroxy alcohol propylene glycol (PG, 1,2-propanediol), which has an identical carbon backbone as C3OH but does not display a Debye-type process that is slower than the structural α-relaxation [15]. In this context, it is interesting to notice that the values T_{on}=364 K and T_A=358 K in PG [14] are much closer to each other than the values T_{on}=311 K and T_A=238 K in C3OH. The onset of cooperative and collective dynamics on cooling seems to occur in C2OH and C3OH at the temperature T_{on} where hydrogen-bonded structures are formed, and not at the temperature T_A where alkyl-chain dynamics produces low-temperature non-Arrhenius behavior of viscosity. This discrepancy seems to relate to the specific chainlike form of hydrogen-bonded aggregates and the corresponding heterogeneous structure in monohydroxy alcohols.

By examining the discrepancy between T_A and T_{on} further, we also considered the temperature T^* at which $\eta(T^*)$=1.5 mPa·s is satisfied because T^* was found to match T_A for organic molecular glass-formers, irrespectively of material [34,39]. Again, we calculated T^* using the power-law relations from Ref. [31] and found an almost perfect agreement between T^* and T_{on} for all studied alcohols (Fig. 4b). This surprising result again indicates that in monohydroxy alcohols, viscosity starts to deviate from Arrhenius behavior at the temperature T_A, which generally differs from the temperature $T_{on}\approx T^*$, where cooperative and collective dynamics occur.

4. Conclusions

We studied tracer diffusivities of nitroxide radical pDTEMPONE by ESR spectroscopy in the series of normal alkanes from octane to tridecane and that of normal alcohols from methanol to 1-octanol. Temperature dependences of radical diffusivities were compared to those of self-diffusivities to determine whether the radical diffusivities in these liquids exhibit the crossover phenomenon detected in the six glass-forming solvents in Ref. [14]. The alkanes, as non-glass-forming liquids, showed the same crossover behavior in which the radical diffusivities being lower than the self-diffusivities at high temperatures approach the self-diffusivities upon temperature lowering. Additionally, the onset temperatures of radical diffusion crossover T_{on} in alkanes correspond well with the Arrhenius crossover temperatures T_A estimated from viscosity, which was also found to hold for the studied glass-forming solvents except for ethanol [14]. The correspondence between T_{on} and T_A indicates the same origin of both crossover phenomena, which is ascribed to the beginning and rise of correlated and cooperative diffusive motion of molecules by cooling liquids below these temperatures.

We found it interesting to compare radical diffusion behavior in alkanes and alcohols because these liquids have similar molecules. However, the alcohols possess the glass-forming ability and exhibit heterogeneous structure due to the separation of polar domains with hydrogen-bonded hydroxyl groups and non-polar domains with alkyl tails. Radical diffusion in the studied alcohols, like in alkanes and other glass-forming liquids [14], was found to be slower than the self-diffusion at high temperatures and to exhibit the crossover phenomenon by cooling. However, we found three major differences between the crossover phenomenon in alcohols and alkanes: (*i*) the low-temperature radical diffusivity in alcohols starts to significantly exceed the self-diffusivity by increasing alkyl-chain length from methanol to 1-octanol, (*ii*) the crossover temperatures T_{cr} are higher in alcohols when compared with the melting temperatures T_m, and (*iii*) the onset temperature T_{on} in alcohols does not generally agree with the Arrhenius crossover temperature T_A estimated from the temperature dependence of viscosity.

The peculiar finding (*i*) that the guest molecule in alcohols is less mobile than the host molecule at high temperatures and more mobile at low temperatures could not be explained solely by the increase of molecules' correlated and cooperative diffusive motion without invoking the existence of hetero-structure in alcohols. We proposed the picture based on experimental results [15,16,27-29], where different mobility regions exist in alcohols at low temperatures due to their hetero-structure: the alkyl chains, being in the non-polar domains, perform fast but restricted diffusive motion about temporally fixed hydroxyl groups in hydrogen-bonded aggregates, while the releasing of the hydroxyl group from one aggregate and joining to another one is slower diffusive motion. This slower diffusive motion governs self-diffusion. It is expected that radical diffusive motion couples with both types of motion in the cooperative and collective diffusion processes at low temperatures, which makes the radical diffusion slower than the local diffusion

of alkyl chains but faster than self-diffusion. As non-polar domains increase in size with increasing alkyl-chain length, the effect of coupling between radical and alkyl-chain diffusive motion increases and enhances radical diffusivity relative to self-diffusivity, which is experimentally observed. At high temperatures, the hydrogen-bonded aggregates are thermally destabilized, and solvent molecules behave as free entities without the difference in the mobility of alkyl chains and hydroxyl groups. As the single-molecule diffusion process prevails at high temperatures, the effect of different sizes and masses of radical and solvent molecules on their diffusivities becomes stronger. By applying the Stokes-Einstein law for the radical and self-diffusivities in this case, we reproduced the experimental result that the radical diffuses slower than solvent molecules at high temperatures.

The finding (*ii*) that the relative temperatures T_{cr}/T_m are higher in alcohols than alkanes can be rationalized by the facts that the relative Arrhenius temperatures T_A/T_m are generally higher in glass-forming liquids than crystallizing ones [34] and that the relative Arrhenius temperatures T_A/T_g are generally higher for glass-forming liquids with hydrogen bonds than other molecular glass-forming liquids [12]. The unexpected finding (*iii*) that the onset temperature T_{on} deviates from the Arrhenius crossover temperature T_A in alcohols was checked against available literature data for lower alcohols. Since the temperature T^* at which viscosity equals 1.5 mPa·s was found to match T_A for organic molecular glass-formers [34,39], we calculated T^* in alcohols and found excellent agreement between T_{on} and T^*. Both findings indicate that the onset temperature of non-Arrhenius viscosity behavior T_A in monohydroxy alcohols is generally not the same as the temperature $T_{on} \approx T^*$ where cooperative and collective dynamics occur. This unexpected behavior is probably related to a specific chainlike form of hydrogen-bonded aggregates in monohydroxy alcohols, but further examinations are needed.

Since radical diffusivity in alcohols exhibits a strong temperature crossover, presumably due to the existence of hetero-structure, we also considered the effect of this crossover on the radical diffusivity close to room temperature, which could have a practical interest. We found that the crossover behavior causes the deviation of room-temperature radical diffusivity from the Stokes-Einstein law and exhibits a strong positive dependence on the alkyl-chain length of alcohols. This finding can be related to the experimental fact that the positive deviation of room-temperature diffusivities of neutral solutes from the Stokes-Einstein law increases much stronger with decreasing the relative solute to solvent size in alcohol solvents than non-polar solvents [3,32,33].

Acknowledgments

This work is supported by the Croatian Science Foundation (Project No. IP-2018-01-3168) and NSF RUI (Grant No. 1856746). The work of doctoral student J. S. has been fully supported by the "Young researchers' career development project - training of doctoral students" of the Croatian Science Foundation.

References

[1] O. Suárez-Iglesias, I. Medina, M. de los Ángeles Sanz, C. Pizarro, J. L. Bueno, *Self-diffusion in molecular fluids and noble gases: available data*, J. Chem. Eng. Data 60 (2015) 2757-2817, DOI: 10.1021/acs.jced.5b00323.

[2] X. Wang, Y. Chi, T. Mu, *A review on the transport properties of ionic liquids*, J. Mol. Liq. 193 (2014) 262-266, DOI: 10.1016/j.molliq.2014.03.011.

[3] A. Kaintz, G. Baker, A. Benesi, M. Maroncelli, *Solute diffusion in ionic liquids, NMR measurements and comparisons to conventional solvents*, J. Phys. Chem. B 117 (2013) 11697-11708, DOI: 10.1021/jp405393d.

[4] T. Yamaguchi, *Coupling between translational diffusion of a solute and dynamics of the heterogeneous structure: higher alcohols and ionic liquids*, J. Phys. Chem. B 126 (2022) 3125-3134, DOI: 10.1021/acs.jpcb.2c01053.

[5] B. Berner, D. Kivelson, *The electron spin resonance line width method for measuring diffusion. A critique*, J. Phys. Chem. 83 (1979) 1406−1412, DOI: 10.1021/j100474a012.

[6] Yu. N. Molin, K. M. Salikhov, K. I. Zamaraev, *Spin exchange principles and applications in chemistry and biology*; Springer-Verlag: Berlin, 1980.

[7] K. M. Salikhov, *Contributions of exchange and dipole-dipole interactions to the shape of EPR spectra of free radicals in diluted solutions*, Appl. Magn. Reson. 38 (2010) 237-256, DOI: 10.1007/s00723-010-0128-x.

[8] B. L. Bales, M. Peric, *EPR line shifts and line shape changes due to spin exchange of nitroxide free radicals in liquids*, J. Phys. Chem. B 101 (1997) 8707-8716, DOI: 10.1021/jp970995g.

[9] D. Merunka, M. Peric, *Measuring radical diffusion in viscous liquids by electron paramagnetic resonance*, J. Mol. Liq. 277 (2019) 886-894, DOI: 10.1016/j.molliq.2019.01.006.

[10] R. Richert, K. Samwer, *Enhanced diffusivity in supercooled liquids*, New J. Phys. 9 (2007) 36, DOI: 10.1088/1367-2630/9/2/036.

[11] H. Sillescu, *Heterogeneity at the glass transition: a review*, J. Non-Cryst. Solids 243 (1999) 81-108, DOI: 10.1016/S0022-3093(98)00831-X.

[12] A. Jaiswal, T. Egami, K. F. Kelton, K. S. Schweizer, and Y. Zhang, *Correlation between fragility and the Arrhenius crossover phenomenon in metallic, molecular, and network liquids*, Phys. Rev. Lett. 117 (2016) 205701, DOI: 10.1103/PhysRevLett.117.205701.

[13] Y. S. Elmatad, D. Chandler, J. P. Garrahan, *Corresponding states of structural glass formers*, J. Phys. Chem. B 113 (2009) 5563-5567, DOI: 10.1021/jp810362g.

[14] J. Slade, D. Merunka, M. Peric, *Radical diffusion crossover phenomenon in glass-forming liquids*, J. Phys. Chem. Lett. 13 (2022) 3510-3515, DOI: 10.1021/acs.jpclett.2c00305.

[15] R. Böhmer, C. Gainaru, R. Richert, *Structure and dynamics of monohydroxy alcohols - Milestones towards their microscopic understanding, 100 years after Debye*, Phys. Rep. 545 (2014) 125-195, DOI: 10.1016/j.physrep.2014.07.005.

[16] Y. Zhai, P. Luo, M. Nagao, K. Nakajima, T. Kikuchi, Y. Kawakita, P. A. Kienzle, A. Faraone, *Relevance of Hydrogen Bonded Associates to the Transport Properties and Nanoscale Dynamics of Liquid and Supercooled 2-Propanol*, Phys. Chem. Chem. Phys. 23 (2021) 7220-7232, DOI: 10.1039/d0cp05481j.

[17] A. Martinelli, M. Marechal, A. Ostlund, J. Cambedouzou, *Insights into the interplay between molecular structure and diffusional motion in 1-alkyl-3-methylimidazolium ionic liquids: a combined PFG NMR and X-ray scattering study*, Phys. Chem. Chem. Phys. 15 (2013) 5510-5517, DOI: 10.1039/C3CP00097D.

[18] J. C. Araque, C. J. Margulis, *In an ionic liquid, high local friction is determined by the proximity to the charge network*, J. Chem. Phys. 149 (2018), 144503, DOI: 10.1063/1.5045675.

[19] D. Merunka, M. Peric, *An analysis of radical diffusion in ionic liquids in terms of free volume theory*, J. Chem. Phys. 152 (2020) 024502, DOI: 10.1063/1.5138130.

[20] F. Castiglione, G. Saielli, M. Mauri, R. Simonutti, A. Mele, *Xenon dynamics in ionic liquids: a combined NMR and MD simulation study*, J. Phys. Chem. B 124 (2020) 6617-6627, DOI: 10.1021/acs.jpcb.0c03357.

[21] P. J. Griffin, Y. Wang, A. P. Holt, A. P. Sokolov, *Communication: Influence of nanophase segregation on ion transport in room temperature ionic liquids*, J. Chem. Phys. 144 (2016) 151104, DOI: 10.1063/1.4947552.

[22] Y. Wang, G. Wang, J. Yao, H. Li, *Restricting Effect of Solvent Aggregates on Distribution and Mobility of CuCl2 in Homogenous Catalysis*, ACS Catal. 9 (2019) 6588-6595, DOI: 10.1021/acscatal.9b01723.

[23] X.-Y. Zhao, L.-N. Wang, Y.-F. He, H.-W. Zhou, Y.-N. Huang, *Measurements and analyses of the conductivities of probe ions in monohydroxy alcohol liquids*, Chem. Phys. 528 (2020) 110473, DOI: 10.1016/j.chemphys.2019.110473.

[24] D. Merunka, M. Peric, *Continuous diffusion model for concentration dependence of nitroxide EPR parameters in normal and supercooled water*, J. Phys. Chem. B 121 (2017) 5259−5272, DOI: 10.1021/acs.jpcb.7b02550.

[25] K. M. Salikhov, A. Ye. Mambetov, M. M. Bakirov, I. T. Khairuzhdinov, R. T. Galeev, R. B. Zaripov, B. L. Bales, *Spin Exchange Between Charged Paramagnetic Particles in Dilute Solutions*, Appl. Magn. Reson. 45 (2014) 911−940, DOI: 10.1007/s00723-014-0571-1.

[26] T. Salez, J. Salez, K. Dalnoki-Veress, E. Raphaël, J. A. Forrest, *Cooperative Strings and Glassy Interfaces*, P. Natl. Acad. Sci. USA 112 (2015) 8227−8231, DOI: 10.1073/pnas.1503133112.

[27] C. Gainaru, R. Meier, S. Schildmann, C. Lederle, W. Hiller, E. A. Rössler, R. Böhmer, *Nuclear-Magnetic-Resonance Measurements Reveal the Origin of the Debye Process in Monohydroxy Alcohols*, Phys. Rev. Lett. 105 (2010) 258303, DOI: 10.1103/PhysRevLett.105.258303.

[28] C. Lederle, W. Hiller, C. Gainaru, R Böhmer, *Diluting the hydrogen bonds in viscous solutions of n-butanol with n-bromobutane: II. A comparison of rotational and translational motions*, J. Chem. Phys. 134 (2011) 064512, DOI: 10.1063/1.3549123.

[29] S. Schildmann, A. Reiser, R. Gainaru, C. Gainaru, R. Böhmer, *Nuclear magnetic resonance and dielectric noise study of spectral densities and correlation functions in the glass forming monoalcohol 2-ethyl-1-hexanol*, J. Chem. Phys. 135 (2011) 174511, DOI: 10.1063/1.3647954.

[30] Y. H. Zhao, M. H. Abraham, A. M. Zissimos, *Fast calculation of van der Waals volume as a sum of atomic and bond contributions and its application to drug compounds*, J. Org. Chem. 68 (2003) 7368−7373, DOI: 10.1021/jo034808o.

[31] M. H. Ghatee, M. Zare, L. Pakdel, *An insight into the dynamic crossover phenomenon in alcohols from the fluidity equation*, Fluid Phase Equilib. 336 (2012) 98−103, DOI: 10.1016/j.fluid.2012.08.027.

[32] D. Fennell Evans, T. Tominaga, C. Chan, *Diffusion of Symmetrical and Spherical Solutes in Protic, Aprotic, and Hydrocarbon Solvents*, J. Solution Chem. 8 (1979) 461−478, DOI: 10.1007/BF00716005.

[33] D. F. Evans, T. Tominaga, H. T. Davis, *Tracer Diffusion in Polyatomic Liquids*, J. Chem. Phys. 74 (1981) 1298−1305, DOI: 10.1063/1.441190.

[34] N. V. Surovtsev, *On the glass-forming ability and short-range bond ordering of liquids*, Chem. Phys. Lett. 477 (2009) 57−59, DOI: 10.1016/j.cplett.2009.05.078.

[35] A. V. Lesikar, *On the self-association of the normal alcohols and the glass transition in alcohol-alcohol solutions*, J. Solution Chem. 6 (1977) 81−93, DOI: 10.1007/BF00643434.

[36] V. A. Zykova, N. V. Surovtsev, *Inelastic Light Scattering Study of Hydrogen-Bonded Glass Formers: Glycerol and Ethanol*, J. Non-Cryst. Solids 471 (2017) 429−434, DOI: 10.1016/j.jnoncrysol.2017.06.036.

[37] F. Stickel, E. W. Fischer, R. Richert, *Dynamics of glass-forming liquids. II. Detailed comparison of dielectric relaxation, dc-conductivity, and viscosity data*, J. Chem. Phys. 104 (1996) 2043−2055, DOI: 10.1063/1.470961.

[38] P. Sillrén, A.Matic, M. Karlsson, M. Koza, M. Maccarini, P. Fouquet, M. Götz, T. Bauer, R. Gulich, P. Lunkenheimer, A. Loidl, J. Mattsson, C. Gainaru, E. Vynokur, S. Schildmann, S. Bauer, A. Loidl, *Liquid 1-propanol studied by neutron scattering, near-infrared, and dielectric spectroscopy*, J. Chem. Phys. 140 (2014) 124501, DOI: 10.1063/1.4868556.

[39] C. Hansen, F. Stickel, R. Richert, E.W. Fischer, *Dynamics of glass-forming liquids. IV. True activated behavior above 2 GHz in the dielectric α-relaxation of organic liquids*, J. Chem. Phys. 108 (1998) 6408−6415, DOI: 10.1063/1.476063.

Graphical Abstract

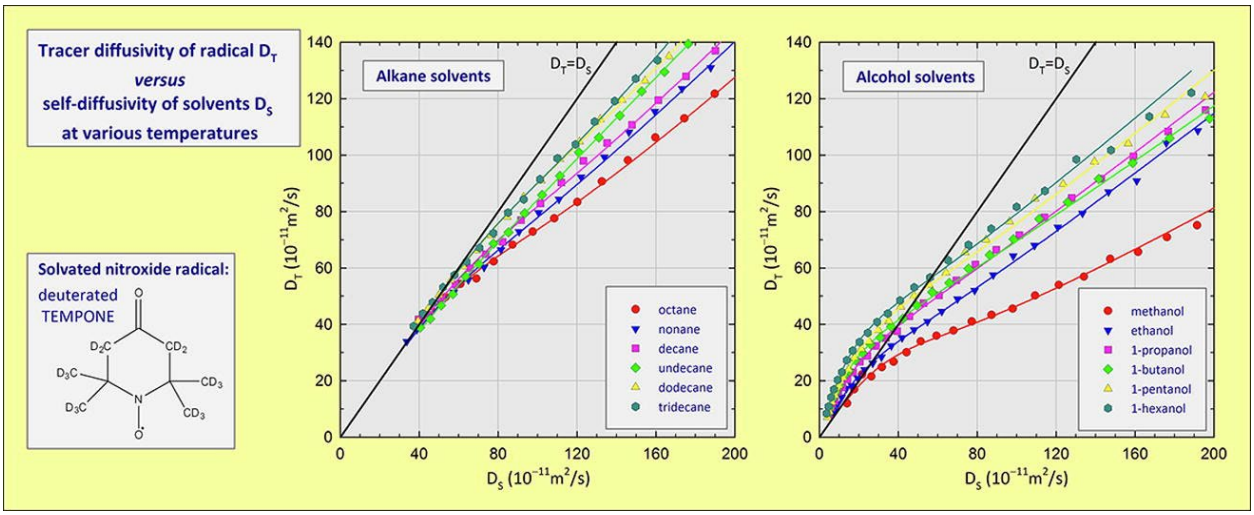

Highlights

- tracer diffusivity of TEMPONE radical in liquid alkanes and alcohols was studied by electron spin resonance
- radical diffusivity exhibits temperature crossover behavior when compared to self-diffusivity in all studied liquids
- radical diffusion crossover phenomenon evidences transformation from individual to collective diffusion process by cooling
- differences of radical diffusion crossovers in alcohols and alkanes indicate the effect of heterogeneous structure in alcohols
- crossover can be related to room-temperature diffusivity deviations from Stokes-Einstein law of neutral solutes in alcohols

Supplementary material for

Comparing Radical Diffusion Crossover Phenomena in Alcohols and Alkanes

Jakov Slade, Dalibor Merunka, and Miroslav Peric

Appendix A. Obtaining radical diffusivity from ESR spectral analysis

The absorption ESR spectrum as a function of applied magnetic field B exhibits three and two hyperfine lines for the solutions of ^{14}N- and ^{15}N-labeled nitroxide radicals, respectively. This is because the number of hyperfine lines is $2I$+1, where I is the nuclear spin of nitrogen, having the values 1 for ^{14}N and 1/2 for ^{15}N. In the presence of spin interactions between radicals, the absorption spectrum $R(B)$ for both radicals in the magnetic field units has the form [1-4]:

$$R(B) = J_0 \,\mathrm{Re}\left[\frac{G(B)}{1-\Lambda G(B)}\right];\; G(B) = \sum_{k=1}^{2I+1} \frac{1}{\Gamma_k + \Lambda + i(B - B_k)}\,. \tag{A.1}$$

where J_0 is the intensity, Λ is the spin coherence-transfer rate, Γ_k is the spin dephasing rate of the k-th line, and B_k is the field position of the k-th line. The field positions are $B_{1,3} = B_0 \pm A + S/3$, $B_2 = B_0 - 2S/3$ for ^{14}N-radical and $B_{1,2} = B_0 \pm A/2$ for ^{15}N-radical, where B_0 is the central field of the spectrum, A is the nitrogen hyperfine splitting, and S is the second-order hyperfine shift.

Experimental ESR spectra given by $S(B) = dR(B)/dB$ were fitted to the first derivative of $R(B)$ from Eq. (A.1). The experimental spectra, fitting curves, and residuals for two concentrations of ^{14}N- and ^{15}N-pDTEMPONE in C5OH at 323.15 K are shown Fig. A.1. The concentration dependences of Λ and the average spin dephasing rate $\Gamma = \sum_k \Gamma_k/(2I+1)$ were analyzed at measured temperatures. Because of the spin interactions between radicals, Λ and Γ linearly depend

on radical concentration at low radical concentrations, with the slopes that depend on radical diffusivity (Fig. A.1).

Figure A.1. ESR spectra (black lines), fits (red lines), and residuals (green lines) for 1 and 12 mM solutions of (a) ^{14}N-pDTEMPONE and (b) ^{15}N-pDTEMPONE in C5OH at 323.15 K. Concentration dependences of (c) spin coherence-transfer rate Λ and (d) average spin dephasing rate Γ for ^{14}N- and ^{15}N-pDTEMPONE in C5OH at various temperatures (symbols) and their linear fits (lines).

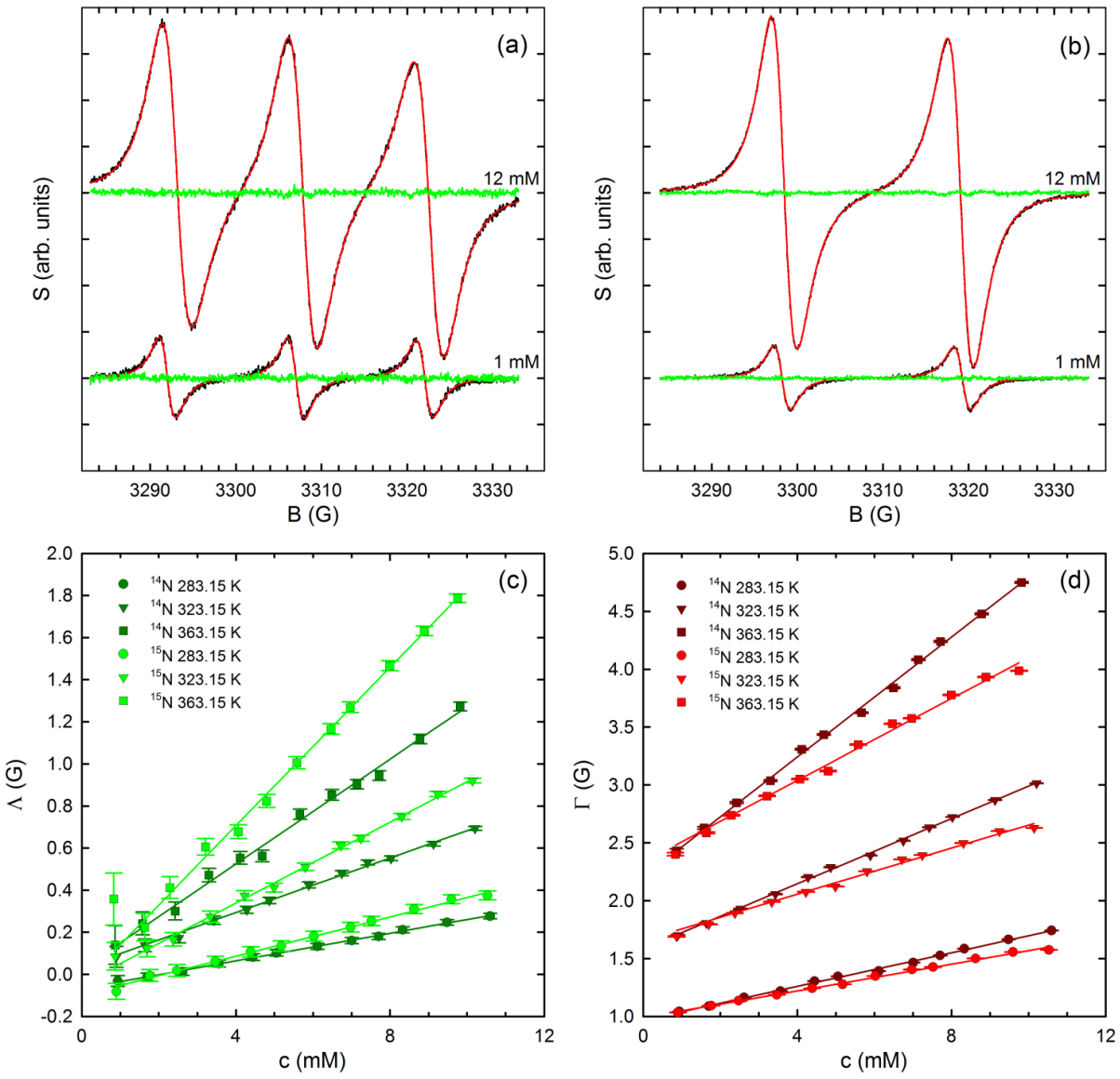

The slopes of Λ and Γ, i.e., their linear concentration coefficients, are denoted as V_j and W_j, respectively, where j is 2 for ^{14}N- and 1 for ^{15}N-pDTEMPONE. The coefficients were calculated by the linear regression method with weights being the inverse squares of standard errors from spectral fitting (Fig. A.1). The temperature dependences of evaluated V_j and W_j for C5OH are shown in Fig. A.2. Theoretical values of the coefficients V_j and W_j were calculated as a

function of radical diffusivity D_T (Fig. A.2) using the continuous diffusion model of rigid spherical radicals and the kinetic equations for spin density matrices of radicals [1-6].

Figure A.2. Experimental values of the concentration coefficients (a) V_j and (b) W_j versus temperature in C5OH (symbols) together with their theoretical values versus radical diffusivity (lines), where j=2 for ^{14}N-pDTEMPONE and j=1 for ^{15}N-pDTEMPONE.

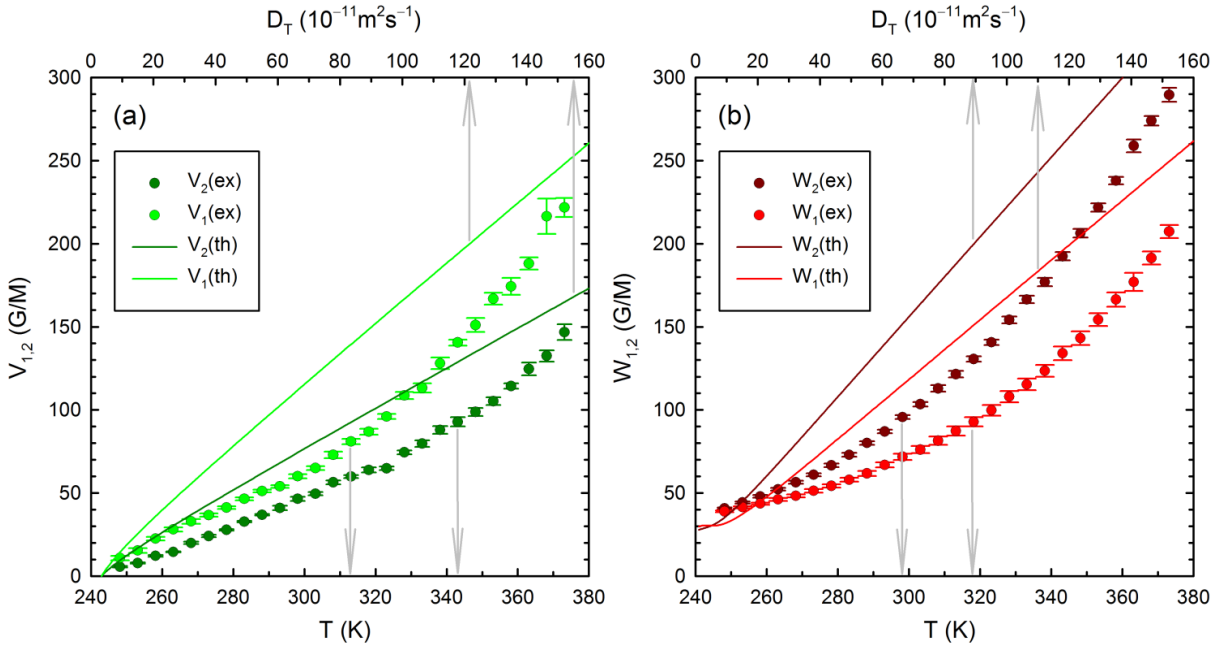

We calculated the corresponding radical diffusivities (Fig. A3) by comparing experimental and theoretical values of the coefficients V_j and W_j. The diffusivities obtained from the coefficients V_j were taken into account for the whole measured temperature range, while those obtained from the coefficients W_j were taken into account for values higher than $25 \cdot 10^{-11}$ m^2 s^{-1} due to saturation at low radical diffusivity [3,7]. The final diffusivities of pDTEMPONE radical presented in Fig.

1 for alkanes and Fig. 2 for alcohols were calculated as the average value of the diffusivities obtained from the coefficients V_j and W_j of ^{15}N- and ^{14}N-labeled radicals (Fig. A.3).

Figure A.3. Temperature dependences of radical diffusivities in C5OH were obtained from the coefficients V_2 and W_2 for ^{14}N-pDTEMPONE and the coefficients V_1 and W_1 for ^{15}N-pDTEMPONE.

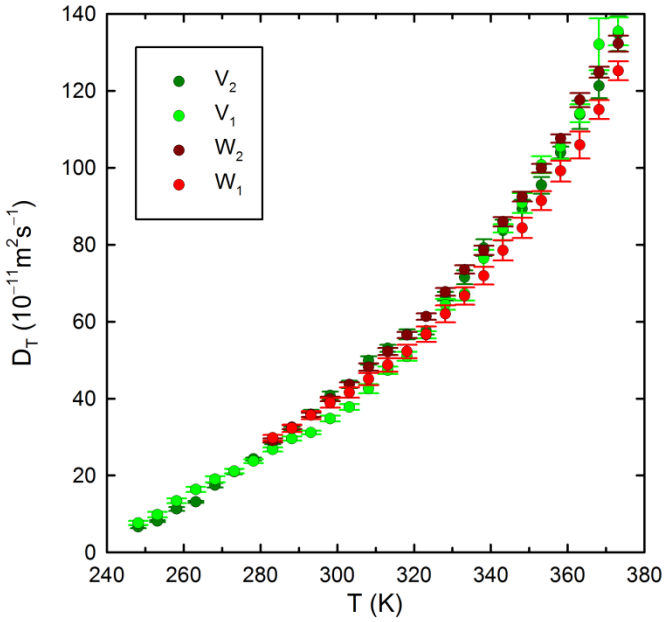

Appendix B. Analysis of self- and tracer diffusivity data

The self-diffusivity values D_S at different temperatures T are shown in Fig. B.1 for studied alkanes and Fig. B.2 for studied alcohols. Data for alkanes contain reported numerical data [8-12] and tabulated data [13] that were read from figures [14-17]. Data for alcohols contain reported numerical data [8,9,18-26], tabulated data [13] that were read from figure [27], and the data read from figure [28]. The references and measured temperature ranges for each liquid are presented in Table B.1. The temperature dependences of self-diffusivities were fitted to the relation:

$$\ln D_S(T) = \ln D_0 - B/(T - T_0), \tag{B.1}$$

which is the Vogel-Fulcher-Tammann law for $T_0>0$ or the Arrhenius law for $T_0=0$. The best-fit values are reported in Table B.1.

Figure B.1. Self-diffusivities vs. temperature in studied alkanes. Symbols denote experimental data, and lines denote the fits to Eq. (B.1).

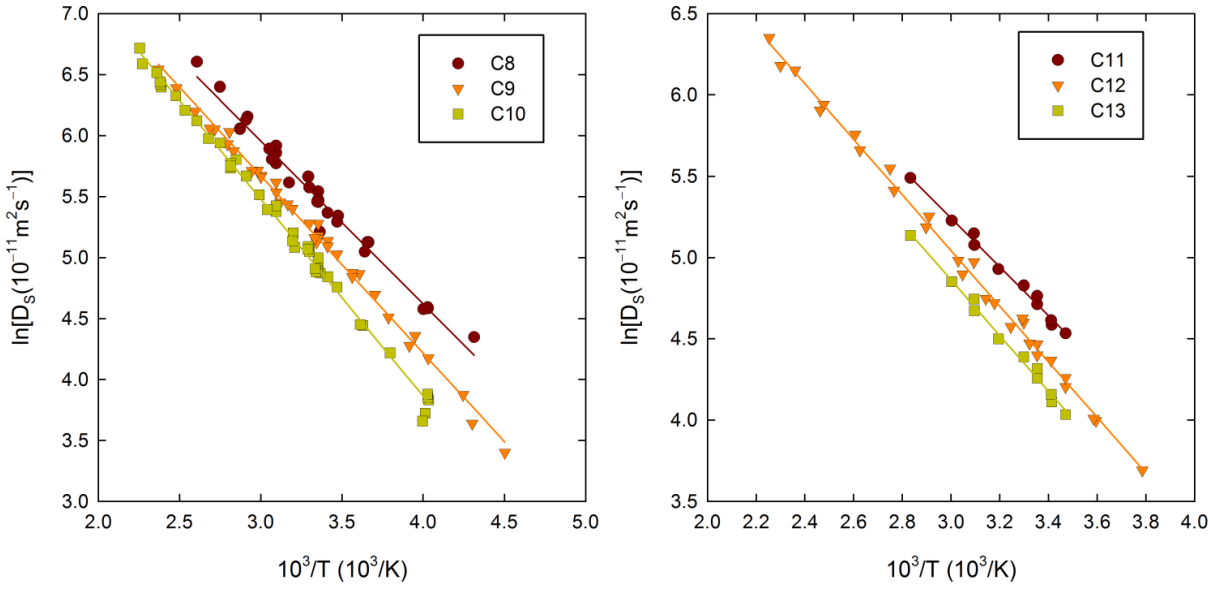

Using the fits $D_S(T)$, which are drawn in Figures B.1 and B.2, temperature dependences of measured tracer diffusivities were fitted to Eq. (1), where the parameter R_L is fixed to 1 for alkanes. The resulting fits $D_T(T)$ are drawn in Figures 1 and 2, while the best-fit values are reported in Table B.2. Also, the temperature ranges of measured radical diffusivities are given in Table B.2, together with the literature values of the melting temperatures T_m of studied liquids.

Fig. B.2. Self-diffusivities vs. temperature in studied alcohols. Symbols denote experimental data, and lines denote the fits to Eq. (B.1).

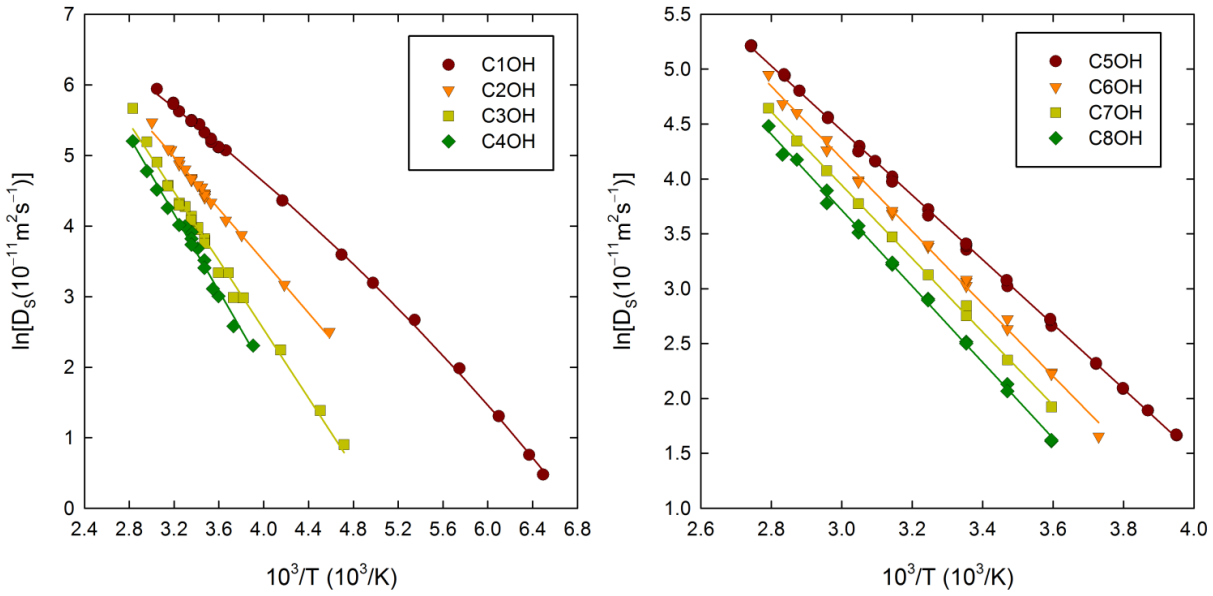

Table B.1. References, measured temperature ranges, and the best-fit parameters from Eq. (B.1) for self-diffusivity data in alcohols and alkanes.

Liquid	References	Temp. range (K)	$\ln[D_0(10^{-11}\mathrm{m^2s^{-1}})]$	B (K)	T_0 (K)
C8	[8-10,13-15]	231-384	9.97	1337	0
C9	[8,9,11,13,14,16,17]	222-422	10.03	1453	0
C10	[8,9,13-16]	247-444	10.33	1616	0
C11	[8,9,11]	288-353	9.74	1498	0
C12	[8,12,13,15,16]	264-444	10.17	1711	0
C13	[8,9,11]	288-353	9.99	1709	0
C1OH	[18-21]	154-329	9.04	880	50
C2OH	[8,13,18-20,27]	218-333	10.86	1840	0
C3OH	[8,13,22,23,27]	212-354	12.26	2432	0
C4OH	[8,23,28]	256-354	12.94	2739	0
C5OH	[12,24,25]	253-365	13.27	2944	0
C6OH	[23,25,26]	268-359	14.08	3298	0
C7OH	[25,26]	278-359	13.95	3337	0
C8OH	[23,26]	278-359	14.09	3459	0

Table B.2. Melting temperatures T_m in studied alkanes and alcohols. Measured temperature ranges and the best-fit parameters R_H, R_L, Δ, and T_{cr} from Eq. (1) for radical diffusivity data. Expected tracer to self-diffusivity ratio from SE law R_{TS}(SE).

Liquid	T_m (K)	Temp. range (K)	R_H	R_L	Δ (K)	T_{cr} (K)	R_{TS}(SE) (K)
C8	216	218-298	0.62	1.00	25	238	0.94
C9	220	223-313	0.69	1.00	29	255	0.98
C10	244	243-323	0.71	1.00	27	275	1.01
C11	248	248-333	0.74	1.00	57	278	1.04
C12	264	263-343	0.79	1.00	27	309	1.07
C13	268	268-353	0.83	1.00	22	313	1.10
C1OH	175	188-324	0.39	0.98	27	219	0.58
C2OH	159	203-334	0.55	1.31	36	248	0.67
C3OH	147	228-354	0.56	1.76	39	272	0.73
C4OH	184	238-374	0.52	2.14	39	281	0.79
C5OH	196	248-374	0.60	1.88	34	301	0.84
C6OH	229	258-374	0.63	2.46	34	303	0.88
C7OH	239	263-374	0.75	1.86	25	323	0.92
C8OH	258	263-374	0.89	2.33	24	320	0.96

Appendix C. Estimation of the Arrhenius crossover temperatures from viscosities

Tabulated data [29] for the temperature dependences of viscosity $\eta(T)$ in studied alkanes [30] and alcohols [31] are presented in Fig. C.1. The temperature ranges of data are reported in Table C.1. In order to estimate the Arrhenius crossover temperature T_A from the viscosity data, we employed the fitting formula [32]:

$$\ln\eta(T) = \ln\eta_0 + E_\infty/(k_B T) + J^2(1/T - 1/T_A)^2\theta(1/T - 1/T_A), \qquad \text{(C.1)}$$

where θ is the Heaviside step function. The fitting formula predicts the Arrhenius temperature dependence above T_A, which is defined by the activation energy E_∞ and pre-exponential factor η_0. The super-Arrhenius behavior below T_A is governed by the parabolic term defined by the parameter J. The best-fit parameter values are presented in Table C.1, and the fits are plotted in Fig. C.1.

Figure C.1. Viscosities vs. temperature in studied liquids. Symbols denote experimental data, and lines denote the fits to Eq. (C.1).

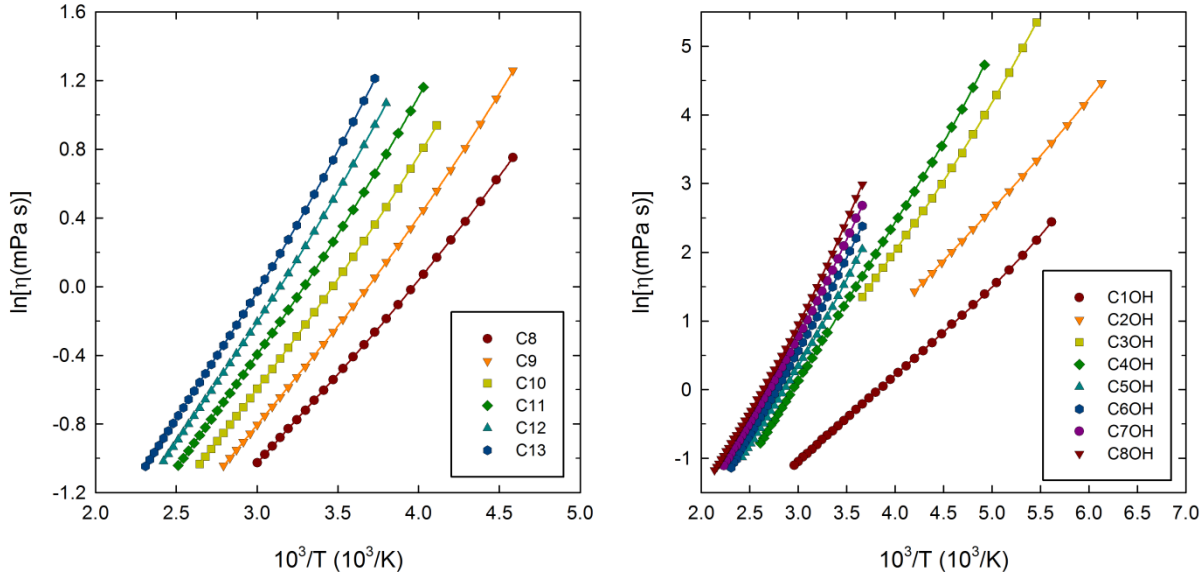

Table C.1. Temperature ranges of analyzed viscosity data in studied liquids and the best-fit values of the parameters, Eq. (C.1).

Liquid	Temp. range (K)	ln[η_0(mPa·s)]	E_∞/k_B (K)	J (K)	T_A (K)
C8	218-333	−4.13	1033	337	288
C9	218-358	−4.25	1147	407	296
C10	243-378	−4.30	1236	412	317
C11	248-398	−4.36	1322	450	328
C12	263-413	−4.39	1394	460	341
C13	268-433	−4.42	1460	484	351
C1OH	178-338	−4.81	1256	464	215
C2OH	163-238	−4.86	1498	344	199
C3OH	183-273	−5.91	1982	525	238
C4OH	203-383	−6.79	2307	721	230
C5OH	273-413	−6.54	2292	637	339
C6OH	273-433	−6.76	2434	539	363
C7OH	273-448	−6.38	2362	607	384
C8OH	273-468	−6.21	2353	697	391

References

[1] K. M. Salikhov, Appl. Magn. Reson. 38 (2010) 237.

[2] D. Merunka, M. Peric, J. Phys. Chem. B 121 (2017) 5259.

[3] D. Merunka, M. Peric, J. Mol. Liq. 277 (2019) 886.

[4] D. Merunka, M. Peric, J. Chem. Phys. 152 (2020) 024502.

[5] J. Slade, D. Merunka, M. Peric, J. Phys. Chem. Lett. 13 (2022) 3510.

[6] K. M. Salikhov, A. Ye. Mambetov, M. M. Bakirov, I. T. Khairuzhdinov, R. T. Galeev, R. B. Zaripov, B. L. Bales, Appl. Magn. Reson. 45 (2014) 911.

[7] B. Berner, D. Kivelson, J. Phys. Chem. 83 (1979) 1406.

[8] P. S. Tofts, D. Lloyd, C. A. Clark, G. J. Barker, G. J. M. Parker, P. McConville, C. Baldock, J. M. Pope, Magn. Reson. Med. 43 (2000) 368.

[9] M. Iwahashi, Y. Yamaguchi, Y. Ogura, M. Suzuki, Bull. Chem. Soc. Jpn. 63 (1990) 2154.

[10] K. R. Harris, J. J. Alexander, T. Goscinska, R. Malhotra, L. A. Woolf, J. H. Dymond, J. Mol. Phys. 78 (1993) 235.

[11] V. P. Arkhipov, Izv. Vyssh. Uchebn. Zaved., Neft Gaz 25 (1982) 34.

[12] M. Holz, S. R. Heil, A. Sacco, Phys. Chem. Chem. Phys. 2 (2000) 4740.

[13] O. Suárez-Iglesias, I. Medina, M. de los Ángeles Sanz, C. Pizarro, J. L. Bueno, J. Chem. Eng. Data 60 (2015) 2757.

[14] D. C. Douglass, D. W. McCall, J. Phys. Chem. 62 (1958) 1102.

[15] E. von Meerwall, S. Beckman, J. Jang, W. L. Mattice J. Chem. Phys. 108 (1998) 4299.

[16] H. Ertl, F. A. L. Dullien, AIChE J. 19 (1973) 1215.

[17] M. Brüsewitz, A. Weiss, Ber. Bunsenges. Phys. Chem. 97 (1993) 1.

[18] N. Karger, T. Vardag, H.-D. Lüdemann, J. Chem. Phys. 93 (1990) 3437.

[19] M. Holz, X. Mao, D. Seiferling, A. Sacco, J. Chem. Phys. 104 (1996) 669.

[20] W. S. Price, H. Ide, Y. Arata, J. Phys. Chem. A 107 (2003) 4784.

[21] R. L. Hurle, A. J. Easteal, L. A. Woolf, J. Chem. Soc., Faraday Trans. 1 81 (1985) 769.

[22] N. Shaker-Gaafar, N. Karger, S. Wappmann, H. D. Lüdemann, Ber. Bunsenges. Phys. Chem. 97 (1993) 805.

[23] M. Petrowsky, R. Frech, J. Phys. Chem. B 114 (2010) 8600.

[24] K. R. Harris, B. Ganbold, W. S. Price, J. Chem. Eng. Data 60 (2015) 3506.

[25] M. Iwahashi, Y. Ohbu, T. Kato, Y. Suzuki, K. Yamauchi, Y. Yamaguchi, M. Muramatsu, Bull. Chem. Soc. Jpn. 59 (1986) 3771.

[26] A. M. Fleshman, G. E. Forsythe, M. Petrowsky, R. Frech, J. Phys. Chem. B 120 (2016) 9959.

[27] S. Meckl, M. D. Zeidler, Mol. Phys. 63 (1988) 85.

[28] C. Lederle, W. Hiller, C. Gainaru, R. Böhmer, J. Chem. Phys. 134 (2011) 064512.

[29] Ch. Wohlfarth, B. Wohlfahrt, *Landolt-Börnstein - Group IV Physical Chemistry, Volume 18B: Viscosity of Pure Organic Liquids and Binary Liquid Mixtures - Pure Organic Liquids*, Springer-Verlag: Berlin, Heidelberg, 2002.

[30] F. D. Rossini, K. S. Pitzer, R. L. Arnett, R. M. Braun, G. C. Pimentel, *Selected values of physical and thermodynamic properties of hydrocarbons and related compounds*, Carnegie Press, Pittsburgh, 1953.

[31] I. F. Golubev, T. M. Pogikhonova, Tr. Gos. Nauchn. Issledov. Proekt. Inst. Azotn. Prom. 8 (1971) 67.

[32] A. Jaiswal, T. Egami, K. F. Kelton, K. S. Schweizer, Y. Zhang, Phys. Rev. Lett. 117 (2016) 205701.